DE-13-032

A Compact Server Model for Transient Data Center Simulations

James W. VanGilder, PE
Member ASHRAE
Christopher M. Healey, PhD
Zachary M. Pardey
Xuanhang Zhang
Member ASHRAE

ABSTRACT

CFD is widely used to determine the steady-state cooling performance of existing or planned data centers. However, in the absence of a compact transient server model, comprehensive transient modeling which includes the effect of server thermal mass requires prohibitively large, detailed models. Consequently, transient scenarios such as that following a loss of cooling are typically modeled in CFD ignoring thermal mass effects of servers (and are thus overly conservative) or are modeled based on a well-mixed idealization, which provides no local information. Further, the techniques used to date for capturing server thermal mass effects in well-mixed models are limited and have not been validated against experimental data.

We propose a compact transient server model that handles all practical data center use cases and is simple to incorporate into CFD, well-mixed, and other numerical models. This black-box server model predicts exhaust temperature in response to time-varying ambient temperature and/or internal heating and can also be used to model entire racks. The model introduces the concept of "server thermal effectiveness" and an additional parameter which takes into account the relative position of server internal heat sources and thermal mass. A method is presented for experimentally measuring the transient server characteristics and preliminary results for sample servers are reported. An example highlights the use of the compact model and its benefits relative to more-approximate techniques.

INTRODUCTION

The importance of data centers to the operation of businesses, the entertainment industry, health care facilities, universities, government institutions, etc., is well known, as is the need to maintain proper cooling to ensure the reliability of servers and other IT equipment housed in such facilities. Data centers also consume a great deal of energy - more than 2% of the power generated in the United States [US EPA 2007] - and supporting infrastructure including cooling often accounts for half or more of the total data center power consumption [Rasmussen 2011]. It is for these reasons that a substantial effort has been directed at the design and operation of data centers including the use of CFD modeling. As evidence of the need and effort, there are at least three data-center-specific CFD tools sold commercially today and several other general-purpose CFD tools are also routinely used for such applications. Furthermore, at least one Data Center Infrastructure Management (DCIM) software package features built-in cooling-modeling technology.

Although CFD is commonly used for modeling a steady-state "snapshot" of the data center, it has not been particularly useful for modeling transient events such as the period of time following a loss of cooling (due, for example, to a power failure in which IT equipment continues to operate on backup power) or load variations due to server virtualization. Consequently, data center designers and operators have only simple hand calculations and "well-mixed" models to "right size" cooling and associated hardware (including UPSs, generators, and supplemental chilled-water storage tanks), plan for power outages, and efficiently operate a dynamic facility. While many aspects of transient CFD modeling, including specifying transient events and including thermal mass of the building

James VanGilder is principal engineer for Cooling Simulation at APC by Schneider Electric, Billerica, Massachusetts. **Zachary Pardey** is a master's student in energy systems at Northeastern University, Boston, Massachusetts and an engineering intern, Cooling Simulation at APC by Schneider Electric, Billerica, Massachusetts. **Christopher Healey** and **Xuanhang (Simon) Zhang** are Senior Engineers, Cooling Simulation at APC by Schneider Electric, Billerica, Massachusetts.

envelope, are fairly straightforward, it is impractical, in a data-center-level simulation, to explicitly model server details to the extent necessary to accurately capture their thermal mass contribution. Yet, we can expect, based on sheer numbers and mass, the server's effect on data center transient temperature changes to be relatively large. Therefore, a compact, black-box model which captures the effect of server thermal mass without additional complication is highly desirable. (Cooling units may also contribute significant thermal mass, for example, in a power-failure scenario when cooling fans and chilled water pumps continue to operate on backup power. However, strictly speaking, it is the circulating chilled water which provides the bulk of the thermal mass. In any event, our attention here is directed at servers, racks, and similar equipment such as UPSs and PDUs.)

Abi-Zadeh and Samain [2001] proposed a well-mixed model in which the entire data center is idealized as a single rack and a single cooling unit. Temperatures, including a single well-mixed air volume, chilled water, and that of various solid objects are computed while including the effects of thermal mass of equipment, chilled water, and, of course, the air itself. Zhang and VanGilder [2011] incorporated this well-mixed model into a tool which allows various cooling-failure modes and backup-power options (for cooling unit fans, circulation pumps, and chillers) to be investigated. Lin and Zhang [2012] then used the well-mixed model to highlight the effects of data center design choices (such as utilizing aisle containment, placing resources on UPS, or incorporating a chilled water thermal storage tank) on transient performance. Khankari [2010, 2011] proposed a simplified well-mixed model in which only the thermal mass of the rack itself (not including its server population) and the air was included. All heat transfer between the rack and the room was assumed to occur through the exposed sides and tops of racks. While this model is very simple, at a minimum, some contribution of server mass would need to be included in order to achieve meaningful accuracy. Sundaralingam et al. [2011] present a well-mixed model for a specific application in which rack inlet and exhaust air is ducted. The thermal mass contribution of the rack, its contents, and other materials within the flow path are included in the analyses. While predictions compare quite well to experimental data, the model is specific to the architecture studied. The well-mixed models are fast and robust but are inherently unable to resolve local effects that are important when data center cooling and equipment layout is highly nonuniform; the single-well-mixed air temperature may or may not be representative of the inlet temperature of any particular rack or server. Furthermore, while the technique of modeling the heat exchange between the air and the thermal mass of the servers only indirectly through the outer skin of the rack (rather than based on airflow through the rack) may provide adequate predictions with appropriate assumptions, it has not been validated experimentally.

Ibrahim et al. [2010, 2012a] first attempted to include server thermal mass in a full data center CFD simulation. The server thermal mass was represented in a semi-explicit manner as heat-dissipating horizontal plates inside a rack which were assigned a density and specific heat to reflect the composition of actual servers. The presence of the thermal mass clearly affected data center temperatures over a range of assumed rack thermal mass loadings. However, the heat exchange between the "server plates" and the air was predicted by the CFD tool rather than specified based on measurements of actual servers. Ibrahim et al. [2011] presented preliminary results aimed at characterizing the thermal mass of a 2U (89 mm) server. Experimental measurements showed the temperature variation of many internal components over time as the server was subjected to varying workload. Ibrahim et al. [2012b] proposed the need for a compact CFD model. They also discussed the importance of characterizing not only the thermal mass itself – commonly thought of as the product of mass and specific heat – but also the internal heat transfer characteristics which determine the heat exchange between the mass of the server and the airflow passing through it.

We build upon the prior work and propose a compact server model that may be directly incorporated into data center numerical models such as CFD. It is a pure, black-box model in the sense that the "parent" CFD model of the surrounding data center need not include any explicit details internal to the server or rack. As the server inlet temperature or rate of internal heating change throughout the transient analysis, the server-exhaust temperature is computed in a manner that comprehends its thermal mass. The model requires the mass and specific heat of the server as input and we detail a few approaches to estimate these quantities for users. It also requires a measure of "server thermal effectiveness," which we introduce to characterize the server's ability to exchange heat with the air passing through it. We will show that thermal effectiveness is more useful than an overall heat transfer coefficient as it restricts input to physically sensible values, varies only very slowly with server airflow rate, and, based on preliminary experimental measurements made here, may be fairly constant over a reasonable range of servers. An additional parameter may optionally be included as input to the compact model; this parameter λ characterizes the position of the heat dissipation in the server relative to the server mass; it is only required when internal server heating changes over time and, even then, we will show that its value may also be fairly consistent across different servers.

Since this compact model is new, we also demonstrate how values for the model's parameters may be estimated with a simple experimental method. While previous methods concerned themselves with server component temperatures (Ibrahim [2011, 2012b]), our experimental method relies only on inlet temperature, exhaust temperature, airflow, and power measurements that can be obtained without accessing the internals of the server. The experimental method detailed in this paper shows how one could measure the transient properties of servers, while also suggesting generally appropriate values which could be used to represent most servers in the

absence of other data. The good agreement between measured and predicted server exhaust temperatures also serves as a validation of the model.

In addition to the development and testing of the model, we discuss how it may be implemented into full data center numerical models and interpreted to represent entire racks. In an example that highlights the importance of proper transient modeling, we consider a range of assumptions from ignoring to including all thermal mass sources. For each assumption, we incorporate our compact transient server model into both CFD and well-mixed models.

DEVELOPMENT OF TRANSIENT SERVER MODEL

An important realization in transient server modeling, stated for the first time here, is that the amount of thermal mass involved in the transient heat transfer process depends on the use case. When the external ambient temperature varies, (e.g., in a data-center-wide loss-of-cooling scenario) the entire server thermal mass is available to moderate server exhaust temperature. Even hot components inside a server, which cannot absorb heat from a cooler airstream, serve as thermal mass. In this case, the "thermal mass effect" of the hot components is not due to the direct absorption of heat from the airstream but rather the reduced rate of heat transfer from the hot component to the airstream. For example, as the ambient temperature increases, the hot component's temperature also increases but more slowly. The resulting lag creates a lower temperature difference between the hot components and the airstream, resulting in a transient server temperature rise that is less than the steady-state value.

When the internal temperature rise varies due to changing server power load or fan speed, the entire thermal mass need not be affected. As an extreme example, imagine the heat-dissipating components as located at the very rear of the server with no upstream heat transfer. Transient changes in power dissipation would not be "seen" by the thermal mass inside the server and the instantaneous transient server temperature rise would be the same as for corresponding steady-state conditions. Of course, not all heat-dissipating components are located at the extreme rear of real servers and a significant amount of heat can be transferred upstream through conduction. In fact, preliminary measurements indicate that the great majority of the server's mass does in fact play a role even for the case where only internal server or power or airflow change with time.

With the above in mind, we construct a server idealization as shown in Figure 1.We imagine a uniformly distributed mass M of uniform temperature T_{eff} with overall effective specific heat $c_{p_{eff}}$. The airstream passing through the server exchanges heat with the thermal mass across a uniformly distributed surface area A and with overall effective heat transfer coefficient h. All server power q_{IT} is added uniformly to the air only (not solid) in a plane located the fractional distance λ along the length of the server. The server ingests air at a rate of $\dot{m}$

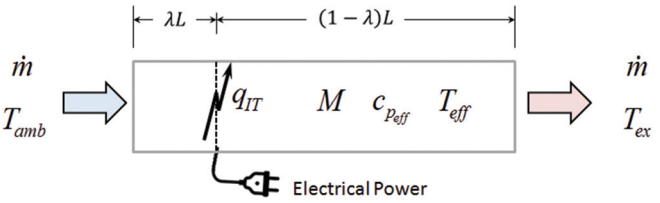

Figure 1 *Server Idealization.*

from the ambient at a temperature of T_{amb} and exhausts airflow at a temperature of T_{ex}.

An instantaneous energy balance over the entire server yields:

$$q_{IT} = Mc_{p_{eff}}\frac{dT_{eff}}{dt} + \dot{m}c_{p_{air}}(T_{ex} - T_{amb}) \qquad (1)$$

where we have assumed that the thermal mass of the air instantaneously located within the server and heat transfer through the sides of the server to the ambient are negligible compared with the other terms in the model. An instantaneous energy balance over a control volume drawn tightly around only the solid mass M (which can be thought of as a uniformly distributed porous media) excluding the heat source isolates the convective heat exchange between the airstream and the solid mass:

$$Mc_{p_{eff}}\frac{dT_{eff}}{dt} = hA_1(T_{amb} - T_{eff}) + hA_2(T_{amb} + \Delta T_{IT} - T_{eff}) \qquad (2)$$

where $\Delta T_{IT} = q_{IT}/\dot{m}c_{p_{air}}$ is the temperature rise across the heat source, h is the heat transfer coefficient, and $A_1 = \lambda A$ and $A_2 = (1-\lambda)A$ are the surface areas of the server mass before and after the server power is added, respectively. In Equation (2) we have assumed, for simplicity, that all of the convective heat transfer to/from the air occurs at uniform air temperatures of T_{amb} and $T_{amb} + \Delta T_{IT}$ upstream and downstream of the heat source respectively. If T_{amb} and ΔT_{IT} were known functions of time, then it would be possible to solve Equations (1) and (2) analytically, in some cases. In a general numerical model of a data center, variations in T_{amb} and ΔT_{IT} are not known in advance, so our approach must yield the correct server exhaust temperature however the ambient temperature or internal server temperature vary. Further, our model must update the server exhaust temperature every time the parent data center numerical model is advanced one time step. We can create a discretized model by approximating the temperature derivative as follows:

$$\frac{dT_{eff}}{dt} = \frac{T_{eff} - T_{eff}^{old}}{\Delta t} \qquad (3)$$

where Δt is the size of the time step and T_{eff}^{old} is the T_{eff} from the previous time step. Solving Equations (1) and (2) and utilizing Equation (3) yields:

$$T_{eff} = \left(\frac{\tau_1}{\tau_1 + \Delta t}\right) T_{eff}^{old} + \left(\frac{\Delta t}{\tau_1 + \Delta t}\right)[T_{amb} + (1-\lambda)\Delta T_{IT}] \tag{4}$$

and

$$T_{ex} = T_{amb} + \Delta T_{IT} + \left(\frac{\tau_2}{\tau_1 + \Delta t}\right)[T_{eff}^{old} - T_{amb} - (1-\lambda)\Delta T_{IT}] \tag{5}$$

where

$$\tau_1 \equiv \text{Server Thermal Time Constant 1} = \frac{M c_{p_{eff}}}{hA} \tag{6}$$

$$\tau_2 \equiv \text{Server Thermal Time Constant 2} = \frac{M c_{p_{eff}}}{\dot{m} c_{p_{air}}} \tag{7}$$

The initial (steady-state) temperature of the thermal mass T_{eff}^0 depends on the location of the heat source and initial values of ambient temperature T_{amb}^0 and temperature rise across the server ΔT_{IT}^0, as follows:

$$T_{eff}^0 = T_{amb}^0 + (1-\lambda)\Delta T_{IT}^0 \tag{8}$$

The corresponding initial server exhaust temperature can be determined from a steady-state version of Equation (1):

$$T_{ex}^0 = T_{amb}^0 + \Delta T_{IT}^0 \tag{9}$$

The thermal time constant τ_1 is defined consistently with traditional lumped-capacitance heat transfer models and represents the relative thermal mass of the server compared to the intimacy of thermal contact between the mass and the air stream. Because the value of hA is server specific, the parameter τ_1 must generally be measured. The thermal time constant τ_2 represents the relative thermal mass compared to the rate at which energy is transported by the airstream. Large time constants imply that the effective server temperature will change slowly over time. As the server thermal time constants approach zero, the server exhaust temperature becomes simply the inlet temperature plus ΔT_{IT}, as expected under steady-state conditions.

We conclude this section with a brief discussion about stability. Since the time step Δt is typically set by the parent numerical model, it is highly desirable that the server transient model remain stable for any arbitrary time step. In can be shown using a method similar to Sucec (1985) that the discretized solution for T_{eff} shown in Equation (4) is stable when $\tau_1 > 0$. Using the same approach, Equation (5) is stable when $\tau_2 > 0$ and $\tau_1 + \Delta t > \tau_2$. Since we desire the solution to be unconditionally stable for any size time step in general, we will require $\tau_1 > \tau_2 > 0$. These conditions and their relation to the 2nd Law of Thermodynamics are discussed further in the following section.

THERMAL EFFECTIVENESS

Equations (4–9) may now be used to estimate the server's effective and exhaust temperatures at each time step in the analysis. Server power q_{IT} and airflow rate $\dot{m}$ are assumed known as required for typical steady-state data center models. The total server mass M and specific heat $c_{p_{eff}}$ can be estimated in a number of ways. Mass may be obtained by weighing servers. Estimates of mass can also be obtained through manufacturers' technical specifications, at least for most base configurations. The specific heat can be estimated through a server "autopsy," but additionally some manufacturers feature component breakdowns which can also provide some insight into the effective server specific heat. Ibrahim et al. [2012b] also states that the specific heat of server components generally fall within a range of 400 to 800 J/(kg °C) (0.1–0.2 Btu/ [lbm °F]), so it may be possible to simply estimate the specific heat of the server as a value within this range. In the Experimental Measurement section, we also suggest an approach to estimate $c_{p_{eff}}$ by fitting the compact model to measured temperature data.

With Δt an arbitrary time step inherited from the parent data center model, we are left only to characterize τ_1 and λ before the model may be implemented. Lacking detailed measurement data for a particular server, the time constant τ_1 may be somewhat difficult to estimate; it is a dimensional quantity (e.g., in seconds), not all values of τ_1 are physically allowable based on 2nd-Law-of-Thermodynamics considerations, and it varies inversely with airflow rate. It is for these reasons we propose an alternative to τ_1, which we call server thermal effectiveness, ε. The effectiveness is a dimensionless number between zero and one; the maximum possible heat transfer between the airstream and the server mass occurs at $\varepsilon = 1$ while zero heat is transferred when $\varepsilon = 0$. Referring again to Figure 1, consider the maximum heat transfer, q_{max}, that can occur between the air stream and the thermal mass (with no internal heating, $\Delta T_{IT} = 0$). From the 2nd Law of Thermodynamics, T_{ex} can never be cooled below or heated above T_{eff} but may approach this value under extreme conditions. Therefore, we define:

$$\varepsilon \equiv \text{Server Thermal Effectiveness} = \frac{q}{q_{max}} = \frac{T_{amb} - T_{ex}}{T_{amb} - T_{eff}} \tag{10}$$

where q is the actual heat transfer between air stream and thermal mass.

We can rewrite Equation (10) as:

$$T_{ex} = T_{amb} + \varepsilon(T_{eff} - T_{amb}) \tag{11}$$

In order to compare this definition of ε with our previously-derived equations, we solve for T_{eff}^{old} in Equation (4) and substitute into Equation (5) (with $\Delta T_{IT} = 0$):

$$T_{ex} = T_{amb} + \frac{\tau_2}{\tau_1}(T_{eff} - T_{amb}) \tag{12}$$

Comparing Equations (11) and (12) yields:

$$\varepsilon = \frac{\tau_2}{\tau_1} = \frac{hA}{\dot{m}c_{p_{air}}} \tag{13}$$

With a clear physical interpretation, server thermal effectiveness ε may be easier to estimate than τ_1 in the absence of measured data. Further, as long as ε is taken between zero and one, physically-sensible input values are assured. Finally, while $\tau_1 = Mc_{p_{eff}}/hA$ varies with server airflow rate, ε remains a weak function of airflow rate as the variations in h and m with airflow rate offset one another. As such, we prefer ε over τ_1 as a transient performance characteristic. At this point, if desired, we could rewrite Equations (4) and (5) in terms of ε and other known parameters.

COMPACT DESCRIPTION OF SERVERS FOR NUMERICAL DATA CENTER MODELS

Relative to steady-state analyses, additional input data required for transient server models are: M, $c_{p_{eff}}$, thermal effectiveness ε, and, possibly, λ. Since the primary value of the model presented here is to include the effects of server thermal mass into a larger data center numerical model, the transient properties will typically be defined in the analysis software as properties associated with a specific server. Figure 2 shows a typical input dialog for capturing the required data. With ε and λ constrained to values between zero and one, it is possible to estimate values based on experience with other servers and is convenient to explore the limit of maximum possible effects of server thermal mass on the overall data center. If ΔT_{IT} remains constant throughout the simulation (i.e., only T_{amb} varies with time), then λ has no effect on server exhaust temperature and may be set arbitrarily. (This independence of λ for external-transient-only scenarios can be shown using Equations (4-9)).

Though not discussed further here, the parent model would, of course, also require a mechanism to input the transient variations of server power and airflow if this were relevant. Most CFD software already provides functionality for specifying the variation with time of many parameters. In addition to the use highlighted in Figure 2, namely in CFD or other detailed analysis tools, the transient model presented here can easily be incorporated into simple well-mixed models like those discussed in Abi-Zadeh and Samain [2001] and Zhang and VanGilder [2011]. The compact model provides such tools with an easy way to account for thermal mass effects.

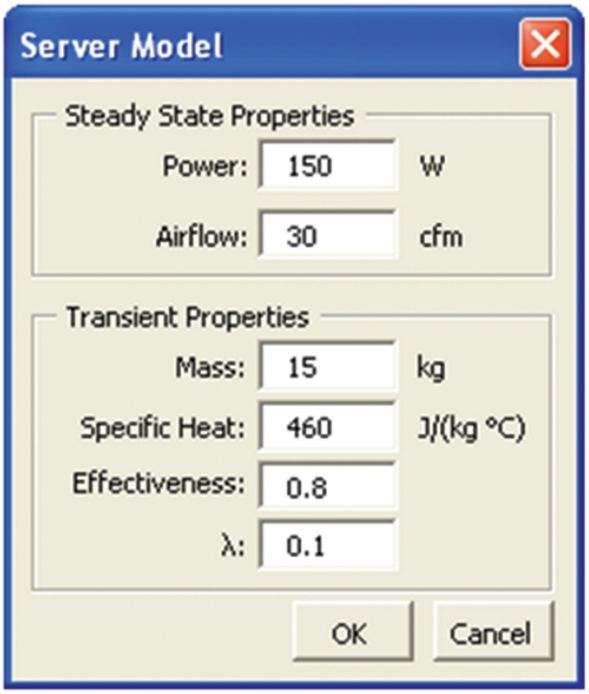

Figure 2 *Input Dialog Box for Capturing Server Properties Required for Transient Analysis.*

AN EXAMPLE ANALYTICAL SOLUTION

Before discussing experimental measurements to determine the transient characteristics of actual servers, we first consider an example, in which the governing equations of our idealized model, Equations (1-2), can be solved analytically. The analytical result, even for a specific example, provides us with a depth of understanding that is difficult to achieve directly from the discretized model. Additionally, we can verify our discretized results for the same case against the analytical model and demonstrate that it provides sensible answers even at large time steps.

In our example, we assume that both the external ambient T_{amb} and internal temperature rise ΔT_{IT} increase linearly starting at time $t = 0$, as follows:

$$T_{amb} = T_{amb}^0 + \alpha t \tag{14}$$

$$\Delta T_{IT} = \Delta T_{IT}^0 + \beta t \tag{15}$$

where α and β are known, positive constants. Substituting these values of T_{amb} and ΔT_{IT} into Equation (2) and solving for T_{eff} yields:

$$T_{eff} =$$

$$T_{amb}^0 + (1-\lambda)\Delta T_{IT}^0 + [\alpha + \beta(1-\lambda)]\left[t - \tau_1\left(1 - e^{\frac{-t}{\tau_1}}\right)\right]$$

(16)

Substituting Equations (14-16) into Equation (1) and solving for T_{ex} yields:

$$T_{ex} = T^0_{amb} + \Delta T^0_{IT} + (\alpha+\beta)t - \tau_2[\alpha+\beta(1-\lambda)]\left(1-e^{\frac{-t}{\tau_1}}\right) \quad (17)$$

We note that λ appears as a coefficient of β, confirming that λ is influential only as internal heating or airflow changes. Also, τ_1 appears in the exponential term, consistent with the role played by the thermal time constant in traditional lumped capacitance heat transfer models.

We can also utilize the analytical results of Equations (14-17) in a graphical manner. Recalling that $\tau_1 = \tau_2 / \varepsilon$, Figure (3a) shows the effect of server thermal effectiveness with $\alpha = \beta = 0.05$ °C/s (0.09°F/s), $\tau_2 = 350$ s, and $\lambda = 0.1$. As ε increases, more heat can be stored by the server thermal mass which results in a lower exhaust temperature. Further, as $\varepsilon \to 0$, the exponential term in Equation (17) vanishes and the exhaust temperature rises with slope equal to $\alpha + \beta$. Figure (3b) shows the effect of λ with the same fixed values as before but now with $\varepsilon = 0.6$ and λ variable. As $\lambda \to 0$, more and more thermal mass is accessible to the changing internal temperature rise. (Recall that, λ only affects the server exhaust temperature when the internal server temperature rise varies and that λ has no effect on the exhaust temperature changes due to ambient temperature variations.)

The analytical results of Equations (16) and (17) also allow us to comment briefly on the discretization scheme proposed for general applications. Figure 4 shows a comparison of the analytical and discretized model results for the fixed parameters used in Figure 3 with $\varepsilon = 0.6$ and $\lambda = 0$. The discretized model matches the analytical result closely for almost all time steps and, as a result, we have to magnify a small portion of the plot to find any discernible differences. While the relative difference is practically insignificant for many time steps, the discretized T_{ex} points do experience a small lag for very large time steps (which is a result of the approximated derivative). These lags decrease as time steps are reduced. In any event, our transient model has to match the parent model – with same time step, so we believe, in practice, our discretization will provide a level of accuracy as high as that of the parent model.

EXPERIMENTAL MEASUREMENT OF TRANSIENT SERVER CHARACTERISTICS

To use our model for practical scenarios, we require estimates of ε and λ for each server in the data center. We know that the entire mass of the server "sees" variations in external ambient temperature but that only the server mass downstream of the server heat source is affected by variations in internal server temperature rise. In other words, when ΔT_{IT} remains constant, λ is arbitrary and has no effect on T_{eff} or T_{ex}. Consequently, we can characterize ε and λ in independent experiments by individually varying T_{amb} and ΔT_{IT} respectively.

Figure 5 shows both a schematic and a photograph of the experimental apparatus used for determining both ε and λ. Inlet and exhaust ducts straighten the airflow and provide repeatable locations at which airflow and temperature measurements are made. A heater is placed upstream of the inlet duct to control the ambient temperature ramp. The exhaust duct contains a straightening section into which is placed several layers of screen, which help smooth out the velocity variations at the server exhaust. Temperature

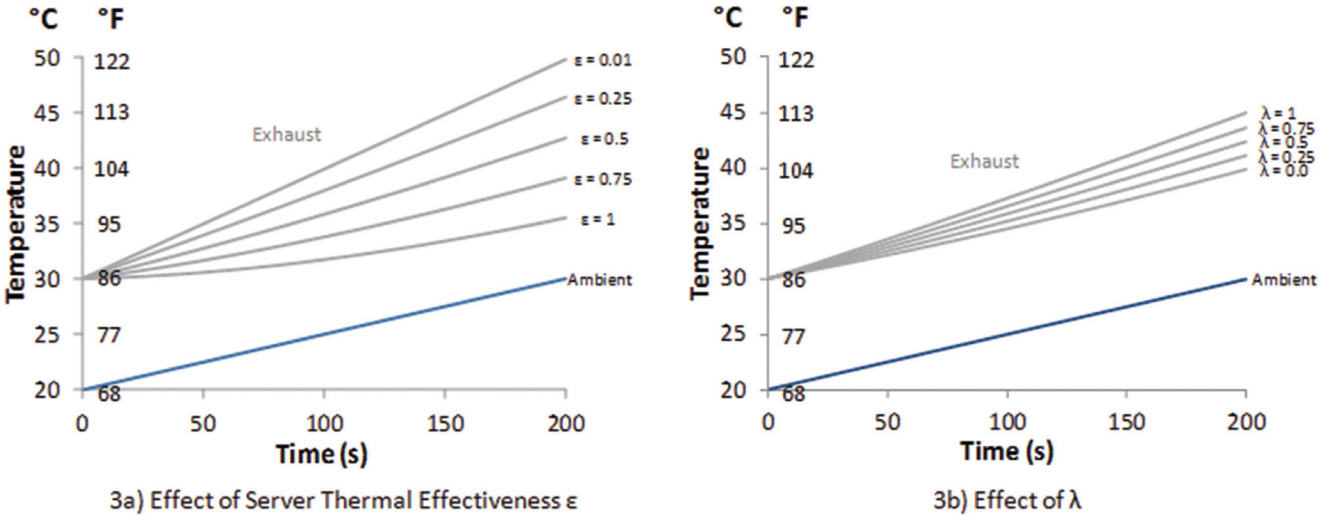

Figure 3 *Effect of Transient Server Model Parameters.*

measurements within the inlet and outlet duct are obtained from an evenly spaced row of thermocouples, as shown in Figure 5a. The actual test apparatus is shown in Figure 5b, with thermal insulation (which would otherwise surround the server chassis) removed for clarity. Velocity measurements are made with a handheld hot wire anemometer whose tip is inserted into locations across the width of the inlet and outlet ducts. Instantaneous power measurements are recorded with a meter reading overall server power, and temperature measurements are logged over time with an automated data acquisition system. Future work will aim to improve airflow control and measurement through the use of a flow bench and refined experimental technique. We will also aim to catalog the thermal mass properties of a reasonable range of contemporary server products for use in general data center modeling. The preliminarily results presented here are intended only as representative examples.

Our measurements attempt to resolve the transient effects embodied in the last term in Equation (5), as distinct from the steady-state temperature rise embodied in the second term. Consequently, we must start with a well-calibrated steady-state model. We base airflow rate measurements on the velocities taken in the inlet duct (as inlet velocities are more uniform than exhaust velocities) with no heat source. Additionally, we calculate the measured exhaust temperature as a weighted sum of the temperature measurements at the exhaust thermocouple locations to account for the fact that the airflow rates at all locations are not necessarily equal. We weight the exhaust temperature measurements as follows:

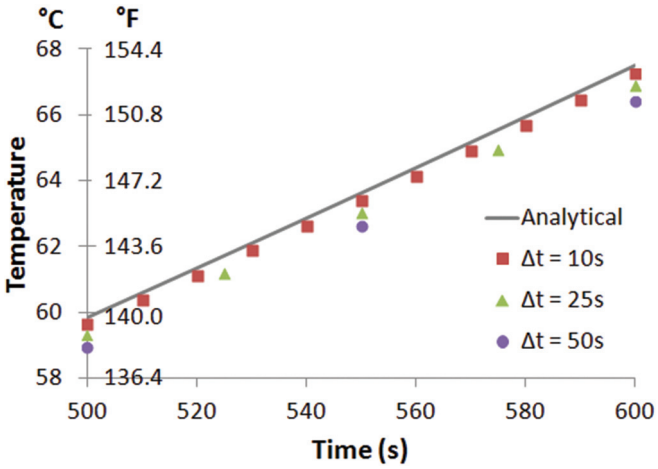

Figure 4 *Comparison of Analytical and Discretized Models.*

$$T_{ex} = a\frac{\sum_{i=1}^{n} V_i T_i}{\sum_{i=1}^{n} V_i} \tag{18}$$

where the V_is and T_is are the measured velocities and temperatures at the exhaust at sensor location i and a is an additional calibration parameter used to empirically correct for measurement error. The parameter a is simply chosen to adjust the right hand side of Equation (18) to match the steady-state T_{ex}^{0} of Equation (9). In our experiments, a fell between 0.94 and 1.13. Following this steady-state calibration step, all measured exhaust temperatures during the transient experiment are computed via Equation (18), while the model-predicted exhaust temperatures are determined with Equations (4) and (5).

Figure 6a shows the measured data and compact model curve fit associated with ε for one of our three test servers, a 1U-Dell R210 server. We start with the server operating under steady conditions then increase T_{amb} in an approximately linear manner by adjusting the aperture of a rectangular slot cut into an insulating wall located between the heater and the inlet duct. The inlet temperature is allowed to level off around 40°C (104°F). Temperatures and server power are recorded with a data acquisition system at approximately 11-second intervals. So that we do not have to measure airflow rate continuously, all three servers considered here are manipulated to run at maximum fan speeds for the entire duration of all trials. (As noted above, ε does not vary significantly with airflow anyway.) In a post-measurement analysis, with our assumed-known M and c_p, we vary ε (or τ_1) until the compact model provides the best fit to the measured data, in this case, $\varepsilon = 0.81$. Note that the effect of thermal mass is very obvious in Figure 6a; the inlet temperature increases at a faster rate than the exhaust temperature and actually exceeds it for about 3 minutes. If there were no thermal mass whatsoever, the exhaust temperature would simply remain a fixed temperature rise above the inlet temperature. If $c_{p_{eff}}$ were difficult to estimate, an alternative approach could tune both $c_{p_{eff}}$ and ε within reasonable ranges to provide the best fit to the experimental data.

To determine λ, a second experiment is conducted in which the ambient temperature is held constant while the internal server load is varied by subjecting the CPU to an increased workload via a dedicated software program. Starting at an idle load (in Figure 6b, the starting load is 95W), the CPU load is increased to 117W at a fixed rate, then held constant. The resulting data is shown in Figure 6b along with the best-fit to the model which occurs at $\lambda = 0.06$. The very small value of λ suggests that nearly the entire server mass "feels" the effect of internal heating.

Data for all three servers measured are summarized in Table 1. Perhaps not surprising in light of the efforts made to cool servers, our test samples are fairly efficient at transferring

heat to or from the airstream as evidenced by the relatively large effectiveness values. Further, the three servers each feature a fitted λ close to zero. Although we have conducted only preliminary measurements on a very small server population, we might speculate that λ is, at least, fairly small for typical servers. Future research will address the thermal properties of other important server types (e.g., blade servers and servers larger than 2U (89 mm)). If $\lambda \approx 0$ appears to hold fairly universally, the compact model of Equations (4-9) could be further simplified.

These results further suggest that server properties (on a per-U basis) may not vary much. Further research and testing may illuminate "typical" server values that can be assumed in cases when CFD users do not have the time or equipment required to individually test servers.

TRANSIENT CHARACTERISTICS OF ENTIRE RACKS

Zhai and Hermansen [2012] discuss how steady-state "black box" models of racks can be created which take into consideration the vertical position of each server, adjusting the temperature rise at each horizontal slice of the rack accordingly. The server model presented here can be applied directly in this manner with the appropriate transient server properties

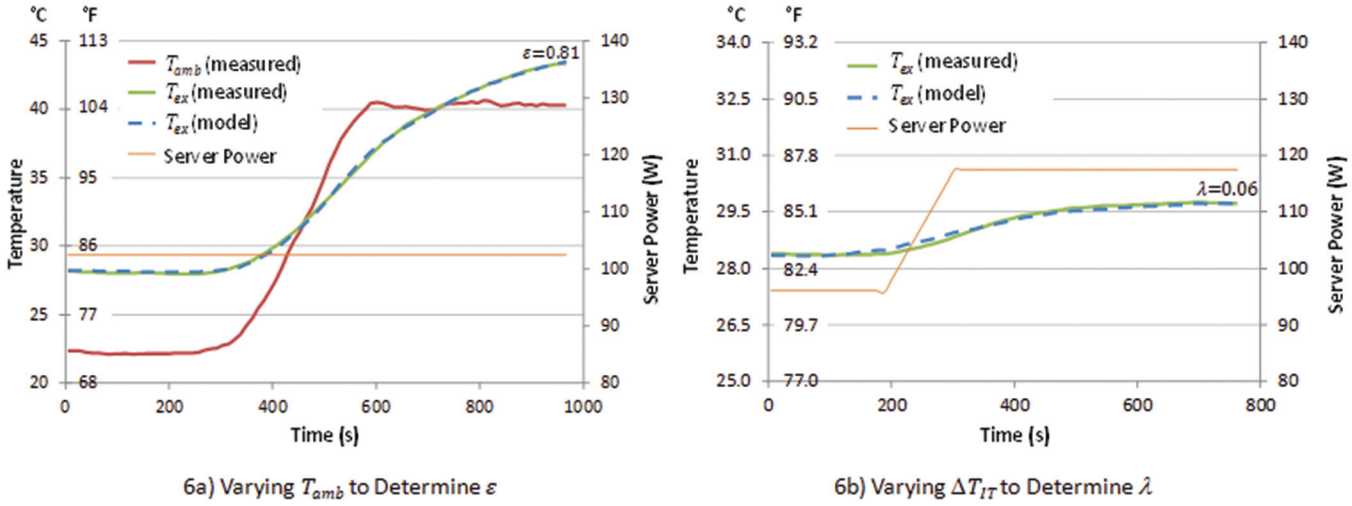

Figure 6 *Measured and Modeled Temperatures for a 1U-Dell R210 Server.*

Table 1. Measured Server Parameters

Server	Q, cfm (L/s)	M, kg (lbs)	$c_{p_{eff}}$, J/kg °C	Ɛ	λ

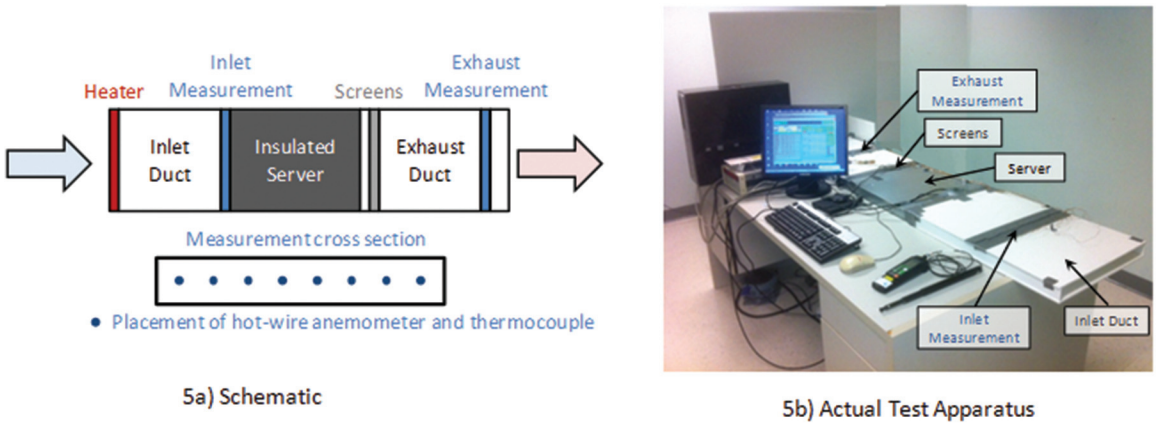

Figure 5 *Experimental Apparatus for Determining Transient Server Properties.*

Table 1. Measured Server Parameters

1U–Dell R210	36 (17)	9.9 (21.8)	480	0.81	0.06
1U–Dell PowerEdge 850	16 (7.6)	6.8 (15.0)	500	0.63	0.01
2U–Dell PowerEdge 2850	60 (28)	20.2 (44.5)	600	0.81	0.03

applied to each slice of the rack; however, it may be unnecessary to include this level of detail given that, at the design stage, specific rack populations are often not well known anyway. In this case, the dialog box shown in Figure 2 may be interpreted to apply to the rack itself and the servers it contains. Of course, if all servers utilized in the rack were identical, rack-based parameters would be easy to compute.

The effective rack-level mass M_{eff}, power $q_{IT_{eff}}$, and airflow $\dot{m}_{eff}$ (or $\dot{Q}_{eff}$ on a volumetric basis) are simply the sum of their server-level counterparts including the rack itself. The effective specific heat can be computed as a mass-weighted average:

$$c_{p_{eff}} = \frac{1}{M_{eff}}\left(\sum_{s=1}^{n} M_s c_{p_s} + M_R c_{p_R}\right) \tag{19}$$

where n is the number of servers and the subscript R refers to the rack itself. Using the definition of thermal effectiveness, $\varepsilon = hA/\dot{m}c_{p_{air}}$, the rack-level effective value can be shown to be:

$$\varepsilon_{eff} = \frac{1}{\dot{Q}_{eff}}\left(\sum_{s=1}^{n} \dot{Q}_s \varepsilon_s + \dot{Q}_R \varepsilon_R\right) = \frac{\sum_{s=1}^{n} \dot{Q}_s \varepsilon_s + \dot{Q}_R \varepsilon_R}{\sum_{s=1}^{n} \dot{Q}_s + \dot{Q}_R} \tag{20}$$

where the airflow rate, $\dot{Q}_R$, and thermal effectiveness, ε_R, of the rack itself are ambiguous. We might guess that ε_R is similar to that of the servers measured here because of the rack's large heat transfer area. In light of this, we suggest that the racks contribution to thermal effectiveness may be ignored (and $\dot{Q}_R = 0$).

Unfortunately, λ_{eff} for the entire rack may, in general, vary with time, making its value somewhat limited. As discussed above, λ may generally be close to zero for many servers making, $\lambda_{eff} = 0$ a reasonable assumption, anyway. However, based on the analytical example presented in Equations (13-17), we suggest that, in the limiting case where all servers have the same time constant $\tau_1 = Mc_{p_{eff}}/hA$ and the same rate of internal heating $\Delta T_{IT}(t)$, λ_{eff} reduces to a heat-capacity-weighted average of the corresponding server values:

$$\lambda_{eff} = \frac{1}{M_{eff} c_{p_{eff}}}\left(\sum_{s=1}^{n} M_s c_{p_s} \lambda_s\right) \tag{21}$$

where $\lambda_R = 0$, as the rack itself does not have any heat sources.

DATA CENTER EXAMPLE

Now that we have discussed the compact transient server model and shown how its required parameters can be determined experimentally, we consider an example implementation to demonstrate its utility. Further, we consider multiple modeling approaches in order to demonstrate the relative importance of server thermal mass to the effects of the building envelope and differences between CFD and well-mixed models.

Figure 7 shows an example data center (33x35x8.5 ft, or 10x10.7x2.6 m) which experiences an abrupt loss of all cooling (all CRAC fans fail) at $t = 0$ while all IT equipment continues to operate as before, powered by UPS. In the interest of a simple, focused example, we ignore any efforts by data center personnel to power-down equipment, open doors, etc. We also ignore any server airflow changes which may occur automatically in response to increasing inlet temperature. The assumed rack

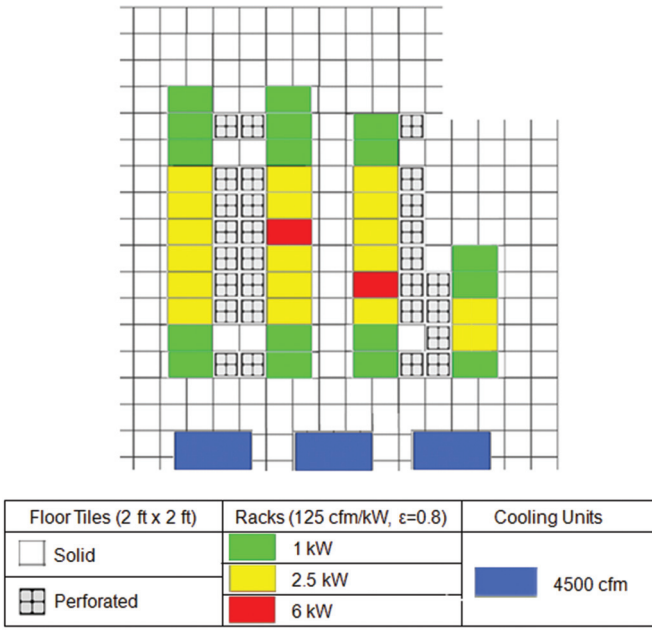

Figure 7 *Transient Example Data Center Layout.*

properties are shown in the legend of Figure 7. We do not require a λ in this example because, as discussed, it has no effect without transient internal server power or airflow variation. The rack mass, specific heat, and thermal effectiveness are based on an assumed full rack of 42 1U-Dell R210 servers (Table 1) and include the rack itself of mass 125 kg (275 lbm) and specific heat 500 J/ (kg °C) (0.12 Btu/[lbm °F]). We realize this is a simplification as, in practice, racks with low heat dissipation will tend to also have smaller mass.

We compare the results of several analyses ranging from a simple well-mixed model in which all solid-object thermal mass is ignored to a CFD implementation of the compact server model which also includes heat transfer through and thermal mass of the building envelope. The former is the simplest transient hand-calculation one might perform and the latter the most sophisticated option now available. We consider three options for modeling solid objects: 1) ignore all heat exchange with solid objects - the air alone absorbs the data center heat load and - treat walls as adiabatic, 2) include heat transfer through and the thermal mass of the building envelope, and 3) include heat transfer through and the thermal mass of the building envelope plus the thermal mass of the racks utilizing the compact model. We model each option 1-3 with both a simple well-mixed model of the type discussed in Zhang and VanGilder [2011] and full CFD for a total of six analyses.

We ignore the thermal mass of the cooling units in all scenarios. In non-adiabatic scenarios, we do not model the raised-floor plenum explicitly but instead assume the floor is fixed at a temperature of 20°C (68°F) in order to simulate heat transfer to and thermal mass of the floor. In the same scenarios, we model the walls and ceiling with a thermal resistance of 0.015 °C/W (0.0079°F/[Btu/hr]) and assume a surrounding ambient temperature of 20°C (68°F). The heat transfer coefficient along the floor, walls, and ceiling is computed in the CFD analyses and, in the well-mixed models, assigned a value of 8W/(m^2 °C) (1.4 Btu/[hft^2°F). The walls are assumed to be 3.18cm (1.25 inch) thick, have an average density of 950 kg/m^3 (59 lbm/ft^3), and a specific heat of 840 J/(kg °C) (0.2 Btu/ lbm°F) which corresponds to standard interior-wall construction.

The commercial CFD software used (FLOVENT v9.3 [2012]) does not directly accommodate the compact transient server model. To implement the model functionally (but inefficiently), we explicitly modeled the inside of the racks as a grid of conducting blocks of specified mass and specific heat. Airflow and heat sources were included and the specified heat-transfer coefficients on the block surfaces were tuned until the exhaust temperatures predicted by CFD matched those of the compact models for a prescribed ambient temperature ramp in a separate analysis of a single isolated rack. The validated rack models were then included in the full example data center model of Figure 7. While this example is intended only to illustrate the use of the compact model, for reference, the standard k- ε turbulence model was used with a nonuniform Cartesian grid. Approximately 772,000 total cells were used with the largest grid cell dimension being approximately 150 mm (6 in) for the scenario including server thermal mass. Thirty variable time steps were used, progressively increasing from 1.7 to 15 seconds over the 300 second period for all scenarios

The two CFD models not including server thermal mass contained 85,500 (nearly uniform) grid cells and each required about 38 minutes on a common dual-core desktop; since these scenarios employed a "black box" model of the racks, we expect similar solution times from simulations which properly incorporate the compact server model. (This is vastly less computational time than would be required if explicit server representations were included. Further, we know of no detailed models that have been experimentally validated, and as such our compact model should be preferable in most cases.)

Figure 8 shows the data center temperatures at mid-rack height at times t = 0, 30, 60 and 300 seconds. We see that, in all cases, the temperatures near the end of the cold aisles tend to rise more quickly, mainly due to recirculation when cooling airflow is lost. We also see dramatic differences in the rate of heating under the three different modeling assumptions. At t = 60 seconds, a majority of racks are already warmer than the ASHRAE allowable limit (ASHRAE [2012]) of 32.2°C (90°F) for adiabatic and building-envelope-only configurations while most of the rack inlet temperatures are well below that threshold when the thermal mass of racks is included. By t = 300 seconds most of the data center exceeds 32.2°C (90°F) even in the most comprehensive CFD model. Including the building envelope's thermal mass noticeably slows the rate of heating of the air relative to ignoring it, while factoring in the thermal mass from racks significantly reduces the rate of heating. The well-mixed model results track their CFD counterparts reasonably well on average but are unable to resolve local temperature variations that may be important.

Table 2 summarizes the time it takes for the average rack inlet temperatures to reach 32.2°C (90°F) under the different modeling assumptions. It can be seen that including the thermal mass of the racks (including their server populations) substantially increases the time to reach the maximum allowable server inlet temperatures. Assuming typical generators require around 30 seconds to start, the thermal mass of the data center can actually maintain acceptable server inlet temperatures during this period of time. Clearly, ignoring the effects of server thermal mass leads to overly-conservative predictions about emergency-condition operating time which makes planning difficult and may drive unnecessary capital expense in the form of quick-start generators, backup power for cooling units, and chilled water storage. The well-mixed models have their place in providing a rough estimate of the time scales over which data center heating occurs, but, are overly optimistic about maximum failure runtime in that they do not recognize the development of local hot spots.

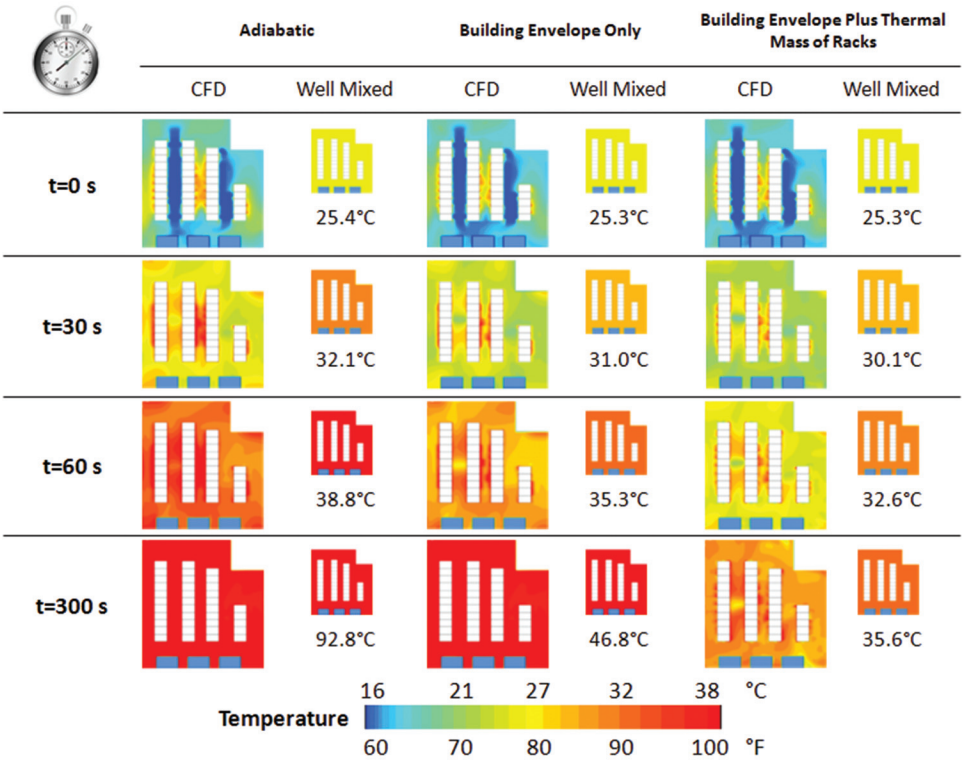

Figure 8 *Temperatures at Mid-Rack Height Following Loss of Cooling.*

Table 2. Time to Reach 32.2°C (90°F) Average Inlet Temperature (seconds)

		Adiabatic	Building Envelope Only	Building Envelope Plus Thermal Mass of Racks
CFD	First Rack	13	17	32
	>50% of Racks	38	46	103
	Last Rack	51	59	241
Well-Mixed		30	56	142

Before concluding this section, we note that, while we didn't include such an example here, the compact transient server model presented here is equally capable of handling non-emergency scenarios in which the rate of server heating changes over time due, for example, to load migration associated with virtualization or server start-up or shut-down. In this case, the server thermal mass may effectively dampen local temperature spikes, providing more time and flexibility in turning on/off cooling units than would otherwise be expected.

SUMMARY AND CONCLUSIONS

We have proposed a simple model for characterizing the thermal response of servers and, by extension, racks, to transient events in the data center or transient changes within the servers themselves. The compact model provides a well-defined and experimentally-validated approach for incorporating effects of server thermal mass in well-mixed models. However, the ultimate value of the model is realized when the compact model is incorporated into numerical models of entire data centers, making it practical to simulate cooling-failure and other transient scenarios in the comprehensive CFD tools upon which designers and operators already rely. While a transient simulation is generally more complex than its steady-state counterpart, the compact model presented here adds essentially no additional computational overhead.

The example provided here showed that including server thermal mass significantly increased the amount of time available to the data center operator following a loss of cooling. It also revealed that, while well-mixed models are capable of

predicting the correct overall transient-heating time scales, they don't reveal local hot spots which could be critical to the operation of the facility.

Relative to steady-state analyses, the additional parameters required by the transient model are the mass M, effective specific heat $c_{p_{eff}}$, server thermal effectiveness ε, and a parameter λ which characterizes the relative location of heat sources within the mass of the server. The parameter λ is only required when the internal server power or airflow vary with time and, even then, preliminary measurements of three servers suggest that $\lambda \approx 0$ may be a generally good approximation. Measured values of thermal effectiveness for the 1U (44.5 mm) and 2U (89 mm) servers considered here were in the range of 0.63 to 0.81. Work remains to measure ε and λ for a broader range of servers and server types as well as other data center equipment such as UPSs and PDUs.

CFD users of tools which accommodate user-defined functions may incorporate the model themselves with only modest effort. If such functions are unavailable, users might construct semi-explicit models as described above, modeling the rack internals as a collection of conducting blocks using a prescribed heat transfer coefficient tuned to provide a match to a measured or assumed server thermal effectiveness. For maximum benefit to the data center community, analysis-software vendors should incorporate this model into their existing server or rack models.

NOMENCLATURE

A	=	Heat transfer area
c_p	=	Specific heat
h	=	Heat transfer coefficient
$\dot{m}$	=	Mass airflow rate
M	=	Mass
q	=	Heat transferred between air stream and thermal mass
q_{IT}	=	Server power dissipation
Q	=	Volumetric airflow rate
t	=	Time
T_{amb}	=	Ambient temperature
T_{eff}	=	Effective server thermal mass temperature
T_{ex}	=	Exhaust temperature
V	=	Velocity
α	=	Constant
β	=	Constant
Δt	=	Time step
ΔT_{IT}	=	Server internal temperature rise
ε	=	Thermal effectiveness
λ	=	Location of power dissipation relative to mass
$\tau_1 = Mc_{p_{eff}}/hA$	=	Time constant (traditional)
$\tau_2 = Mc_{p_{eff}}/\dot{m}c_{p_{air}}$	=	Time constant (secondary)

REFERENCES

Abi-Zadeh, D., and Samain, P. 2001. A transient analysis of environmental conditions for a mission critical facility after a failure of power, arup mission critical facilities.

ASHRAE. 2012. Thermal Guidelines for Data Processing Environments, Developed by ASHRAE Technical Committee 9.9.

Flovent v. 9.3. Software. 2012. Mentor Graphics Corp., 8005 SW Boeckman Road, Wilsonville, OR, USA, http://www.mentor.com.

Ibrahim, M., Afram, F., Sammakia, B., Ghose, K., Murray, B., Iyengar, M., and Schmidt, R. 2011. Characterization of a server thermal mass using experimental measurements, Proceedings of the ASME InterPACK conference, July 6-8, Portland, Oregon, USA.

Ibrahim, M., Bhopte, S., Sammakia, B., Murray, B., Iyengar, M., and Schmidt, R. 2010. Effect of thermal characteristics of electronic enclosures on dynamic data center performance, Proceedings of the ASME IMECE conference, November 12-18, Vancouver, British Columbia, Canada.

Ibrahim, M., Bhopte, S., Sammakia, B., Murray, B., Iyengar, M., and Schmidt, R. 2012a. Effect of transient boundary conditions and detailed thermal modeling of data center rooms, IEEE Transactions on Components, Packaging, and Manufacturing Technology, 2(2), February, pp. 300-310.

Ibrahim, M., Shrivastava, S., Sammakia, B., and Ghose, K. 2012b. Thermal mass characterization of a server at different fan speeds, Proceeding of the IEEE ITherm conference, May 30-June 1, San Diego, California, USA.

Khankari, K. 2010. Thermal mass availability for cooling data centers during power shutdown, ASHRAE Transactions, 116(2).

Khankari, K. 2011. Rate of heating analysis of data centers during power shutdown, ASHRAE Transactions, 117(1).

Lin, P., Zhang, X., and VanGilder, J. 2012. Assessing the risk of data center temperature rise during chilled water cooling loss, White Paper, APC by Schneider Electric. http://www.apc.com/prod_docs/results.cfm?class=wp&allpapers=1.

Rasmussen, Neil. 2011. Electrical efficiency measurement for data centers, White Paper 154, Rev. 2, APC by Schneider Electric. http://www.apc.com/prod_docs/results.cfm?class=wp&allpapers=1.

Sucec, J. 1985. *Heat Transfer*, pp. 260-261. Duquque, Iowa: William C. Brown Publishers.

Sundaralingam, V., Isaacs, S., Kumar, P., and Joshi, Y. 2011. Modeling thermal mass of a data center validated with actual data due to chiller failure, Proceedings of the ASME IMECE conference, November 11-17, Denver, Colorado, USA.

U.S. Environmental Protection Agency ENERGY STAR Program. 2007. Report to congress on server and data center energy efficiency. Public Law 109-431. http://www.energystar.gov/ia/partners/prod_development/downloads/EPA_Datacenter_Report_Congress_Final1.pdf.

Zhai, J. and Hermansen, K. 2012. The development of simplified rack boundary conditions for numerical data center models. ASHRAE. RP-1487.

Zhang, X., and VanGilder, J. 2011. Real-time data center transient analysis, Proceedings of the ASME InterPACK conference, July 6-8, Portland, Oregon, USA.